International Journal of Advanced Technology and Engineering Exploration, Vol 9(88)
ISSN (Print): 2394-5443 ISSN (Online): 2394-7454
http://dx.doi.org/10.19101/IJATEE.2021.874830

Research Article

Numerical investigation of residual stresses in circumferential and longitudinal welded joints

Veeresh B R[1*], R Suresh[2] and Gowreesh S S[1]
Department of Mechanical Engineering, JSS Academy of Technical Education, Bangalore, India[1]
Department of Mechanical Engineering, Siddaganga Institute of Technology, Tumkur, India[2]

Received: 20-September-2021; Revised: 05-March-2022; Accepted: 08-March-2022

Abstract
Welded cylinder structures such as pressure vessels and pipes have found its application in power stations. They experience high temperature and pressure during the operation. As welding induces residual stresses, it is vital to study the stress distribution in predicting their service lives. In the present work, a sequentially coupled thermal structural analysis is carried to study the thermal field distribution and subsequent residual stresses during welding. Finite element (FE) model of gas tungsten arc welding (GTAW) process is developed to produce circumferential and longitudinal butt weld joints of AH 36 (low carbon steel) cylinder components. Welding of cylinders is analyzed by changing their outer diameters. Effect of cylinder outer diameter on residual stresses is studied. The weld induced hoop and axial stresses are evaluated on both inner surfaces (I/S) and an outer surface (O/S) of the cylinder. The magnitude of hoop and axial stresses in longitudinal butt weld joints are 45% and 95% higher than circumferential butt weld joints. By comparing the results, longitudinal butt weld joints are not desirable for fabricating cylinder components. The analysis model is validated with experimental measurements.

Keywords
Welding simulation, Thin-walled cylinder, Thermo-mechanical analysis, Residual stress.

1.Introduction
Welding is a fabrication technique where several variables are involved, which affect the output. Thus, making it a complex manufacturing technique. Welding is being used commonly in power plants, aerospace, marine and pressure vessel applications. Residual stress is one of the detrimental effects which is induced due to welding. Residual stresses induced in the base metals produce distortions such as buckling and bending [1]. The magnitude of peak residual stresses will be in the range of yield strength of the metal. Weld distortions significantly ruin the performance and reliability of the welded components [2]. In case of welded cylinder structures, the residual stress variation and distortion are more complex as it produces axial and circumferential shrinkages in the cylinder. Circumferential and longitudinal welded cylinders are used in piping systems carrying fluids at very high temperature [3].

Circumferential welding is used when cylindrical components are having a diameter equivalent to standard sizes. Cylinder components having diameters other than the standard sizes are fabricated by longitudinal welding of rolled metal sheets. Welding of cylinder structure induces residual hoop and axial stresses, which makes them different from welded flat plates [4, 5]. Weld induced hoop and axial stress distributions depend on the cylinder outer diameter, thickness, welding sequence and procedure [6]. Circumferential and longitudinal weld joints in pressure vessels experience catastrophic failures because of residual stresses. So, it is essential to investigate the residual stress distribution and optimize the welding process parameters. Though experimental methods deliver valuable insights of welding technique, they are complicated and expensive. Numerical approach based on finite element method is an appropriate tool in thermo-mechanical investigation of arc welding process. In this research work, finite element (FE) analysis is carried out to investigate the thermal distribution and residual stresses in circumferential and longitudinal butt weld joints. The primary aim of this study is to

*Author for correspondence

enhance the structural integrity and in-service performance of welded cylinder structures by presenting a comparative study on circumferential and longitudinal butt weld joints. The research work comprises the preparation of FE model of circumferential and longitudinal weld joints. Simulation of the welding arc is carried out using a moving heat source. Temperature profiles and residual axial and hoop stress distributions on the O/S and I/S of the cylinder are investigated.

The current research work is presented as follows: the literature review illustrating the approach of different authors is discussed in section 2. The method employed for the simulation of welding is presented in section 3. The numerical results and its validation are discussed in section 4. The comparative study of the numerical results and limitations are discussed in section 5. Conclusion and the future work are covered in section 6.

2.Literature review

Experimental methods like hole drilling techniques and X-ray diffraction are commonly used to measure the weld induced stresses [7, 8]. Strain gauge rosette was used to measure residual stresses [7]. In that research results show that the axial and hoop stresses are tensile near the weld zone. In the research work [8], the authors defined the procedure for using deep hole drilling and X-ray diffraction method in measuring the residual stresses. They considered butt welding of high grade steel piping systems in power plants in their work. Many numbers of research works are carried out on FE analysis of welding process. Ansys tool was used to predict the weld induced axial and hoop stress in welded pipes [9]. 3D finite element analysis has proved to be more efficient than 2D in predicting the weld induced stresses. The magnitude of residual stress decreased by considering multi pass weld joints. As the number of weld passes increases, the residual stress decreases [10]. Numerical investigations carried out on butt welded pipe joint [11] reported that the plastic compressive strain induced on the I/S of the pipe is higher than O/S. In this work, it is also reported that the residual stresses induced on the I/S of the pipe are tensile. An increase in the outer diameter of the cylinder increases the bending in welded cylinders [12]. Experimental investigations on longitudinally welded pipes revealed the cracks initiated on the I/S of the cylinder, where the residual stresses are tensile and maximum [13]. An investigation on welded line pipes reported that the residual axial stresses initiate fatigue cracks at the weld root [14]. The residual stresses in the girth welded pipes reduces the fracture toughness at the weld region [15]. Failure in the pipe flange weld joint, handling steam at high temperature and pressure was studied [16]. From the investigation, it is found that the higher the magnitude of tensile residual stress and larger size of the grains of the weld root are responsible. Strip samples from circumferential welded pipes can be used for validation in engineering critical assessment results, as no change in the magnitude of residual hoop and axial stresses is observed [17]. The magnitude of residual axial and hoop stress in welded cylinders depend on the material of base metal. Investigation of residual stresses in welded stainless steel and carbon-manganese steel cylinders showed that the magnitude of tensile hoop stress is higher in carbon-manganese steel cylinders [18]. Welding current is one of the important parameters in the welding process. It decides the metal deposition rate and depth of penetration during welding. By increasing the current, the peak temperature during the weld increases [19] and also the residual stress increases [20]. As welding technique affects the in-service performance of the welded structures post weld treatments are carried out. Post weld techniques relieve the residual stresses induced during welding. Weld overlay is one of the post weld technique to reduce the residual stresses. The weld overlay process in low alloy and austenitic stainless steel piping systems reduced the magnitude of residual stress [21]. Also, the length and thickness of the weld overlay have no effect on the induced stresses. Repair welds are the post weld techniques used to join the defects such as cracks initiated by fatigue or corrosion. The repair welds on the welded cylinder structures increased the residual stresses. The magnitude of residual axial stresses increases by larger extend than hoop stresses by repair welds. Even by increasing the length of the repair weld, the magnitude of peak tensile residual stresses is not reduced [22]. Post weld processes like ultrasonic impact treatment induce compressive stress on the surface of the welded components. The induced stresses are compressive up to a depth of 8mm irrespective of the nature of the initial weld induced stress [23, 24]. Post weld heat treatment, like tempering on circumferentially welded cylinder reduced the magnitude of residual stresses [25]. By observing the previous research works, it is found that weld induced residual stresses and distortions are inevitable. Even the repair welds used to cover the cracks induces residual stresses and adds to the previously existing stresses. Some of the post weld techniques like weld overlay, ultrasonic impact

treatment and tampering reduces the magnitude of tensile residual stresses and are expensive. So it is required to select the type of weld which induces lower residual stresses. In this paper, a comparison of thermal histories and residual stresses between circumferential and longitudinal weld joints is carried out. Also, the literature suggests that, with the availability of advanced computer technology, weld induced residual stresses can be predicted more precisely. A numerical study has been conducted to find the temperature variation, maximum temperature and residual stress distributions in circumferential and longitudinal weld joints.

3.Methods

Sequentially coupled thermal structural analysis approach is used in the present work and is as shown in *Figure 1*.

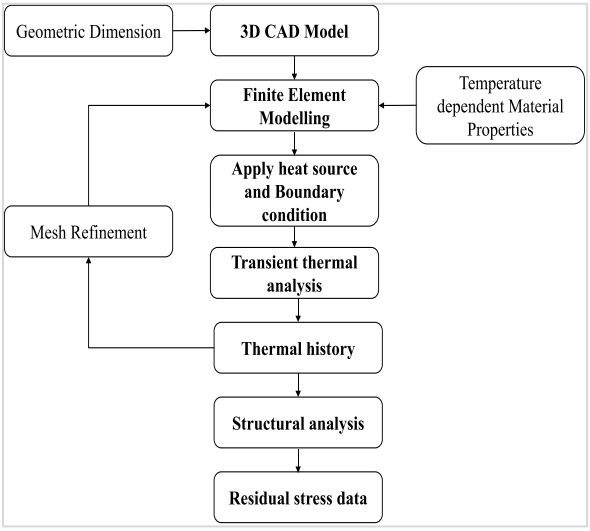

Figure 1 Method followed in the present work

In the first step, an investigation is carried out to measure the thermal cycles during the weld. Thermal histories from the first step are applied as thermal load during structural analysis to determine the residual stress distribution. The analysis of gas tungsten arc welding (GTAW) is carried using commercially available FE software.

3.1FE modelling

To measure the temperature and induced stresses, three dimensional FE models of circumferential and longitudinal butt weld joints are developed. During the analysis of circumferential butt weld joints, two cases having a cylinder outer diameter 300mm (C-300) and 200mm (C-200) are considered. Similarly, for the analysis of longitudinal butt weld joints, two cases having a cylinder outer diameter 300mm (L-300) and 200mm (L-200) are considered. Thus, in total four cases, i.e. C-300, C-200, L-300 and L-200 are considered for analysis. In all the mentioned cases, the length and thickness of the cylinder are 300mm and 3mm, respectively. The dimensions of the weld bead in all the four cases are as shown in the *Figure 2*.

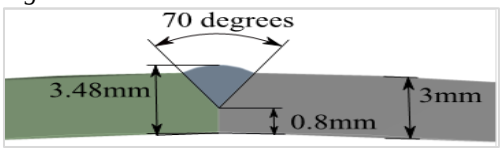

Figure 2 Dimension of the weld bead

The dimension of the weld bead is taken from the experimental study carried by Malik et al. [9]. They have studied circumferential welding on cylinders having dimensions same as the case C-300. *Figure 2* shows V-type of butt welding where the included angle is 70^0. The FE models for C-300 and L-300 after discretization are shown in *Figures 3 and 4*.

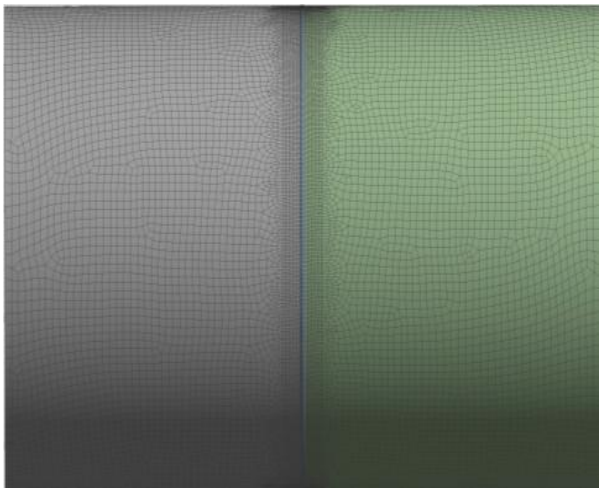

Figure 3 FE model of C-300 after meshing

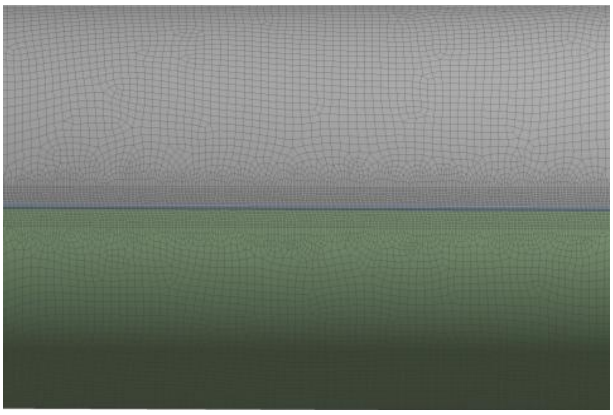

Figure 4 FE model of L-300 after meshing

From the *Figures 3* and *4*, it can observe that the density of the mesh is higher near the weld region. The number of elements on both the cylinder components are same. During FE meshing, 1D linear elements are used to represent the weld line. The line on which the heat source travels are welding line. The free surfaces of the FE model are meshed by 2D quadrilateral elements. Cylinder components and weld bead are meshed by 3D quadrilateral elements. Along the weld line, elements of size 1.8mm are used in all the four cases. For meshing the cylinder components, within a distance of 10mm measured on both the sides of weld line, elements of size 1mm are used. The distance 10mm from weld line is measured in transverse direction. For the other regions of cylinder components, the size of the elements used for meshing is 5mm. Since, thickness of the cylinder is constant in all the cases, three elements, each having a size of 1mm are used along the thickness. Temperature distribution and residual stresses in welded components depend on the material properties. Thus, thermal and mechanical properties at different temperatures are required to get valid results. During the analysis, FE tool uses the material property data as shown in *Figures 5* and *6.*

Figure 5 shows the magnitude of density, thermal conductivity and specific heat at different temperature. *Figure 6* shows the magnitude of elastic modulus, thermal expansion and Poisson's ratio at different temperature.

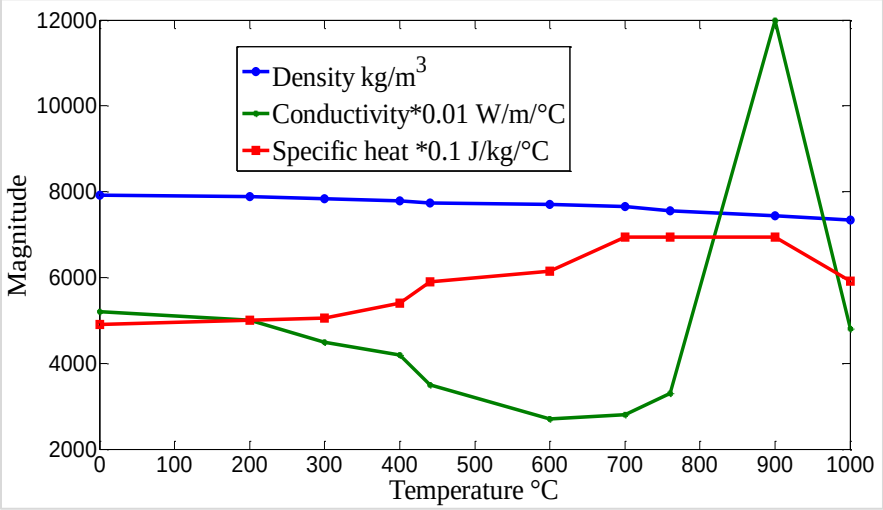

Figure 5 Thermal properties of AH 36

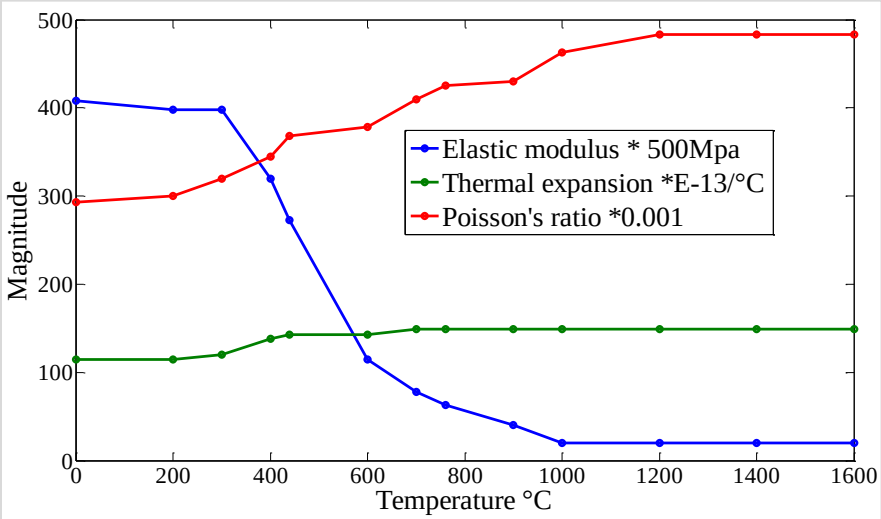

Figure 6 Mechanical properties of AH 36

3.2Thermal model

The thermal analysis is conducted to measure the temperature distributions during the welding process. A double ellipsoid heat source model by Goldak [26, 27] is considered for representing the heat distribution during the welding process. The power density distributions according to Goldak's model are defined by the governing Equations 1 and 2. Equation 1 describes the amount of heat flux in the front portion of the double ellipsoid heat source model. Similarly, Equation 2 describes the amount of heat flux in the rear portion.

$$q_f = \frac{6\sqrt{3}\eta Q h_f}{\pi\sqrt{\pi} a_f bc} \exp\{-3\left(\frac{x^2}{{a_f}^2} + \frac{y^2}{b^2} + \frac{z^2}{c^2}\right)\} \quad (1)$$

$$q_r = \frac{6\sqrt{3}\eta Q h_r}{\pi\sqrt{\pi} a_r bc} \exp\{-3\left(\frac{x^2}{{a_r}^2} + \frac{y^2}{b^2} + \frac{z^2}{c^2}\right)\} \quad (2)$$

Where Q is the magnitude of heat input and is given in the Equation 3. Heat input is the amount of heat energy transferred for unit length. The portions of heat energy placed in the front and rear quadrants are represented by factors h_f and h_r respectively. The magnitude of factors h_f and h_r are 1.25 and 0.75, respectively. The shape and size of the heat source model are defined by arbitrary constants a_f, b, c and a_r. The moving heat source travels on the weld line and the calculated volumetric heat flux density is employed to the elements of FE models. The values of the constants a_f, b, c and a_r in the Equation 1 and 2 are 5mm, 5mm, 3mm and 15mm respectively. The magnitude of heat input during welding depends on the thickness of the base metals. Also, the magnitude of residual stresses induced depends on the magnitude of heat applied. Therefore, parameters such as current and voltage (power) for welding are considered from the work carried by Malik et al. [9]. In their research, an experimental study is carried out on GTAW of cylinder components.

$$Q = \frac{\eta VI}{n} \quad (3)$$

Where I is the current ($2*10^2$A), V is the voltage (12.5V), η is the efficiency of weld (80%) and n is the arc travel speed (3mm/s). Equation 3 describes the amount of heat input during the welding process. During the thermal analysis, both convective and radiative heat loss is considered. Heat is lost by natural convection from all the free surfaces of the FE model. The governing equations for heat loss is given by Equations 4 and 5.

$$q_{loss} = q_{convection} + q_{radiation} \quad (4)$$

$$q_{loss} = [h + \varepsilon\sigma(T + T_{amb})(T^2 + T_{amb}^2)] \times A_s(T - T_{amb}) \quad (5)$$

Where h represents convective heat transfer coefficient (25 W/m^2 ^{0}C), A_s is the surface area (m^2), T_{amb} is ambient temperature (25 ^{0}C), T is the present temperature, σ is Boltzman constant (5.670×10^{-8} W/m^2 K^4), $\mathcal{E}$ is emissivity coefficient (0.8). Equation 4 represents the total heat loss considering both convection and radiation mode. Equation 5 represents the heat lost from the surface of welded cylinder surfaces.

3.3Mechanical model

The successive step after thermal analysis is structural analysis. To find the weld induced residual stresses, structural analysis is conducted. The same FE model after evaluating the temperature distribution is used here. The mechanical properties considered are temperature dependent. Thermal histories of all the nodes during thermal analysis acts as the load input. Von Mises criteria is employed during residual stress evaluation. The boundary conditions applied are the restrictions, which represents the clamps used to fix the cylinder components during welding. The boundary condition applied for C-300 and L-300 is as shown in *Figures 7* and *8*. During the structural analysis, all the nodes on both the edges of the cylinder section are constrained in x, y and z planes. The same boundary condition is being applied in the case of C-200 and L-200. The displacement is restricted in all the directions for the nodes at 00 and 1800 in case of C-300 as shown in *Figure 7*. Locations 00 and 1800 are measured from the weld start location. In case of L-300, displacement of the nodes at 90^0 on both the edges of the cylinder are restricted as shown in *Figure 8*. Location 90^0 is measured from the weld line.

In case of C-300 and C-200, the heat source travels along the circumference of the cylinder. Thus, the weld direction will be normal to the axis of the cylinder. Whereas in the cases L-300 and L-200, the heat source travels along the linear direction parallel to the axis of the cylinder.

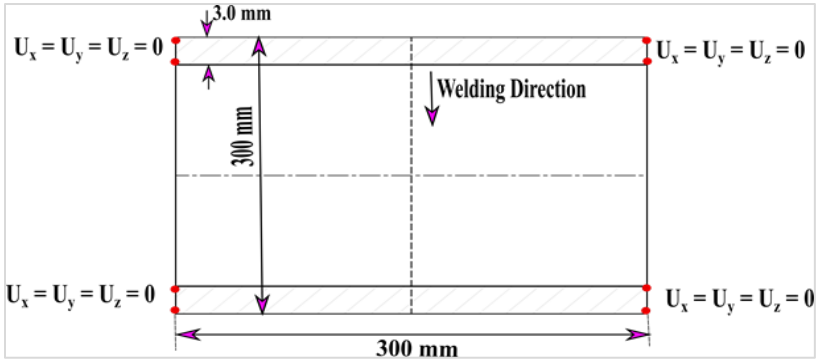

Figure 7 Boundary conditions in case of C-300

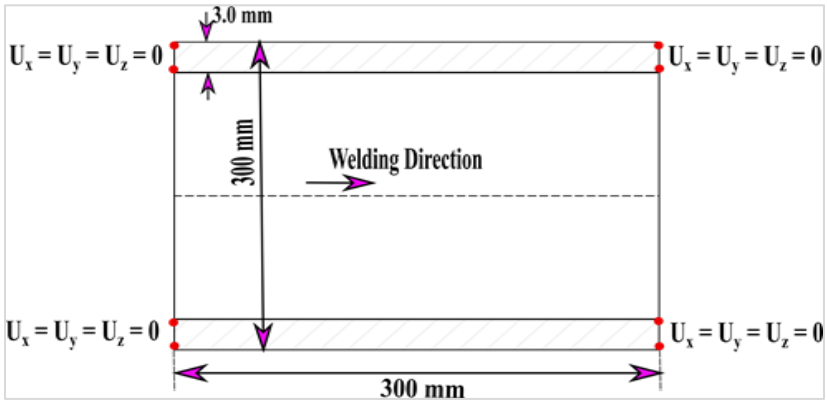

Figure 8 Boundary conditions in case of L-300

4.Results

4.1Validation

The thermal histories and residual stresses from the analysis of C-300 were compared with the experimental measurements available in the work carried by Malik et al. [9]. They have used thermocouples and strain gauges to measure the temperature and residual stresses, respectively. The thermal histories at different time frames are compared. The magnitude of temperatures at two different locations, 10mm and 300; 20mm and 900 for different time frames are considered. The distances 10mm and 20mm are measured in the transverse direction of the weld line. The locations 300 and 900 are measured from the weld start location. Comparing the results, a maximum of 9% variation is observed as shown in *Figure 9.*

From the *Figure 9*, it can be observed that initially the temperature rises to a higher value, showing heat transfer from the moving heat source. After the completion of welding, the temperature gradually reduces with time, showing heat loss from the surface of the cylinder. It is also found that the magnitude of temperatures obtained in case of C-300 is in a close match with the experimental values.

Similarly, the residual stresses are compared as shown in *Figure 10*. The residual stresses at two different locations 450 and 2250 at a distance of 10mm from the weld line are considered. The locations 450 and 2250 are measured from the weld start position.

Figure 10 shows the comparison of residual hoop and axial stresses on O/S of the cylinder at two different locations. A maximum of 40% and 10% variations are observed in the magnitudes of axial and hoop stress, respectively.

The temperature profile and residual stresses from the analysis matches closely with the experimental results, thus the developed FE model is validated.

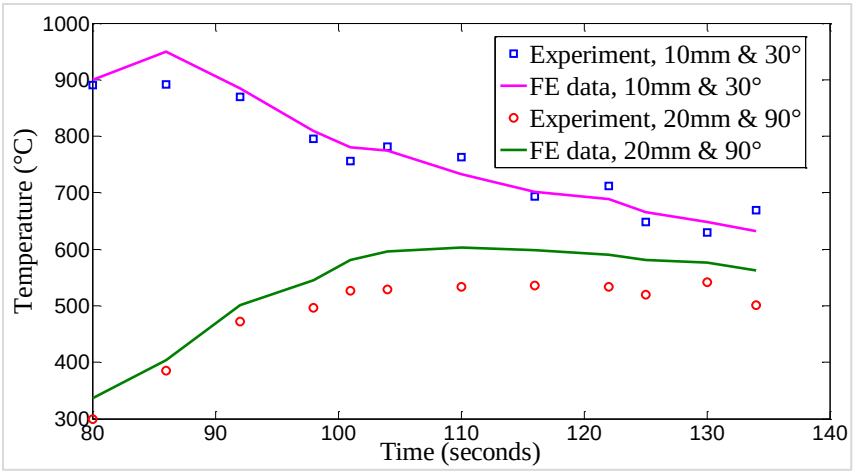

Figure 9 Comparison of thermal histories obtained for C-300 with experimental results

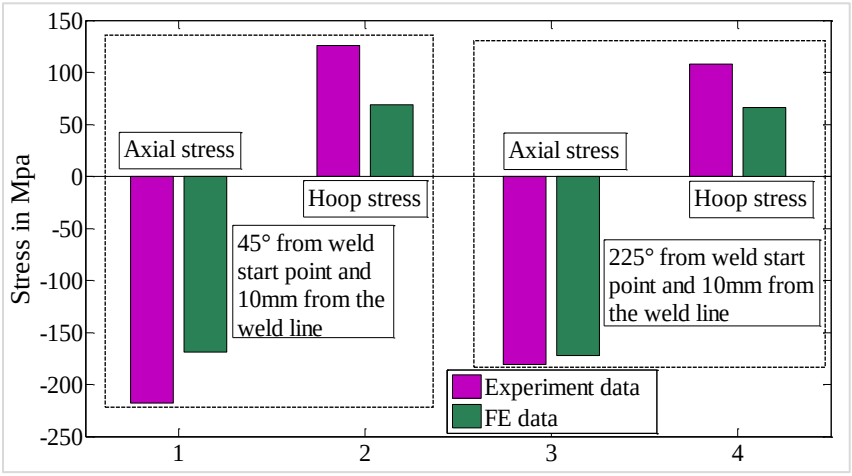

Figure 10 Comparison of residual stresses obtained for C-300 with experimental results

4.2Thermal analysis

With the weld speed of 3mm/s, the heating period along the weld line is 314s in case of C-300. The peak temperature recorded during the welding is 1865.2^{0}C and is observed on the weld line. The peak temperature is recorded at 108s. The temperature variation on the weld line and cylinder components is as shown in the *Figure 11*.

As heat source travels on the weld line, the temperature is maximum on it. Due to heat transfer, the temperature at the regions near to the weld line increases gradually. The gradients trailing the heat source in *Figure 11* indicates the cooling phenomenon of the cylinder components. It can also be observed that the region in front of the heat source is at ambient temperature. Thus, the welding model developed is appropriate.

Figure 12 (a) and *(b)* shows the temperature variation for C-300 at two different time frames. The magnitude of temperatures recorded are 1739.5^{0}C and 1778^{0}C at 78s and 157s, respectively. From the *Figure 12*, it can be observed that the temperature is maximum on the weld line compared to other regions.

As the results from FE analysis are mesh sensitive, refinement is necessary. Sequence of analysis is carried out in case of C-300 by increasing the mesh density. The magnitude of the peak temperature and the corresponding number of elements in each analysis are recorded as shown in *Figure 13*.

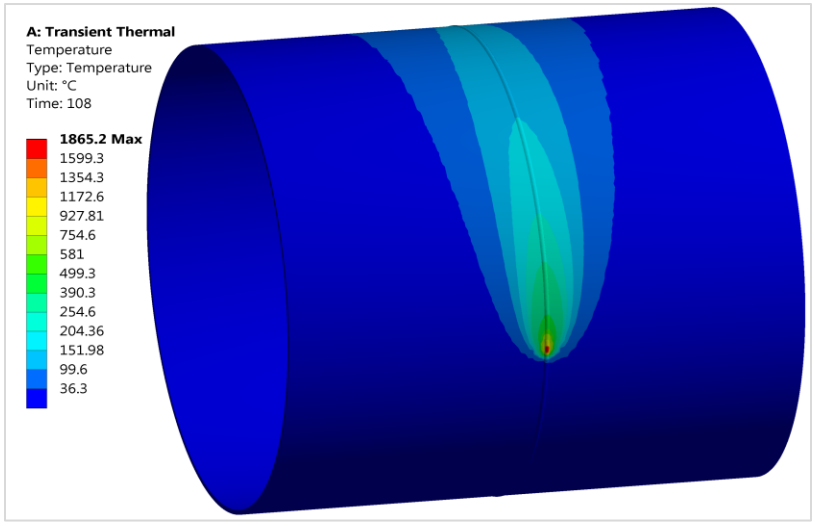

Figure 11 Temperature profile on O/S in case of C-300 at 108s

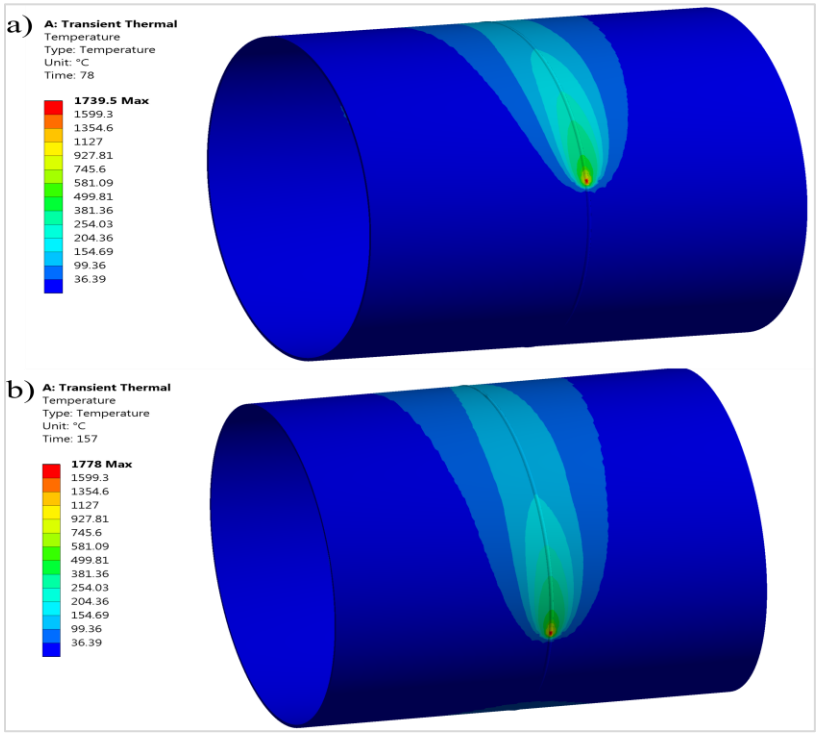

Figure 12 Temperature profiles for C-300 at two different time frames

The peak temperatures recorded during the analysis increased with the increase in the number of elements. The magnitude of peak temperature is found to increase by 40%. From the *Figure 13*, it can be observed that there is no change in the peak temperature above 54090 elements. The FE model developed to analyse the welding in case of C-300, is implemented in L-300 to find the thermal history and residual stress distribution. With heat source travelling at a speed of 3mm/s, it takes 100s to complete welding of 300mm. Peak temperature is recorded at 44s in case of L-300 and is as shown in *Figure 14.*

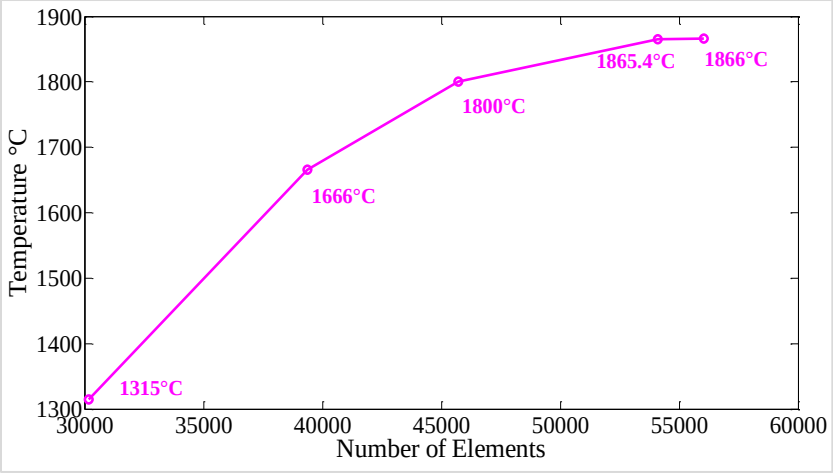

Figure 13 Peak temperatures recorded with respect to the number of elements

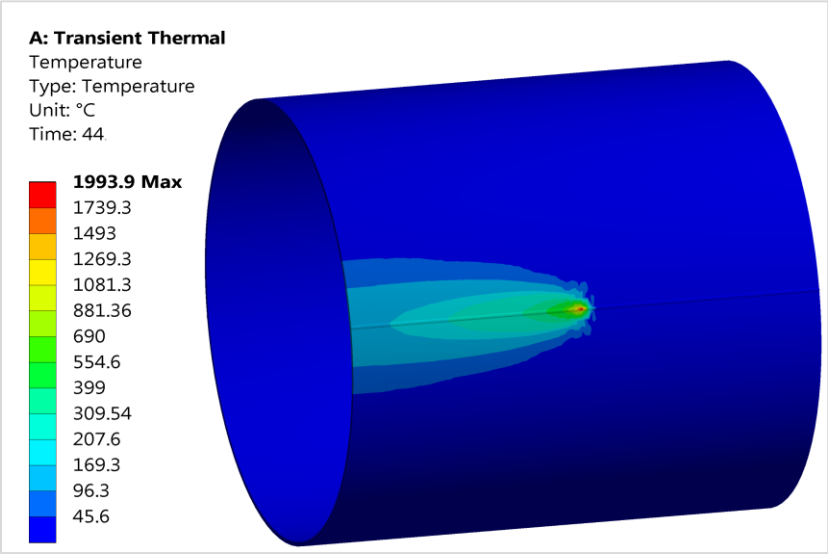

Figure 14 Temperature profile on O/S in case of L-300 at 44s

From *Figure 14*, it can be observed that maximum temperature recorded is 1993.9^0C on the weld line. The maximum temperature on the weld line is because of the heat source.

From *Figures 11* and *14*, it can be observed that the maximum temperatures during the analysis are 1865.2^0C and 1993.9^0C for C-300 and L-300, respectively. Thus, the peak temperature in case of L-300 is higher than C-300. The time taken in case of L-300 to weld half distance, i.e.100 mm, is 100 seconds. Whereas in case of C-300, it takes a time of 157 seconds for the heat source to travel 180^0.

Figure 15 (a) and *(b)* shows the temperature variation for L-300 at two different time frames during the welding process. The magnitude of temperatures recorded on weld line are 1975.3^0C and 1975.6^0C at 25s and 50s, respectively. It can be observed that the temperature is maximum on the weld line compared to other regions.

The temperature variations for C-300 and L-300 at different time frames are shown in *Figures 16* and *17*.

Figure 16 shows the temperature variations in the case of C-300 at location 135^0 for time frames 118s and 196s. The location 135^0 is measured circumferentially from the weld start position on the weld line. Similarly, *Figure 17* shows the temperature variations at 135mm in case of L-300 for time frames 45s and 145s. Distance 135mm is measured axially from the weld start position on the

weld line. In case of C-300, it takes 118s for the heat source to travel 135^0. Whereas in case of L-300 it takes 45s for the heat source to travel 135mm. Because of the heat source, the temperature is maximum on the weld line. The locations away from the weld line are at ambient temperature. At 196s and 145s, the temperature on the weld line decreases due to heat loss in case of C-300 and L-300, respectively. The temperature on the locations away from the weld line increased due to heat transfer. Thus, the temperature is maximum at the welding arc position and decreases as the arc crosses the location. The analysis is carried out for 1800s, so that the complete cylindrical vessel cools to ambient temperature. From the temperature profiles of C-300 and L-300, it is found that the magnitude of peak temperature is higher in case of L-300. By considering the same welding parameters and boundary conditions, FE analysis of C-200 and L-200 is carried out. Since the outer diameter is 200mm in case of C-200 and L-200, the analysis is carried out to find the effect of cylinder outer diameter. In case of C-200, the heat source takes 209.5s to complete the welding. During welding, the peak temperature recorded is at 109s and is shown in the *Figure 18.*

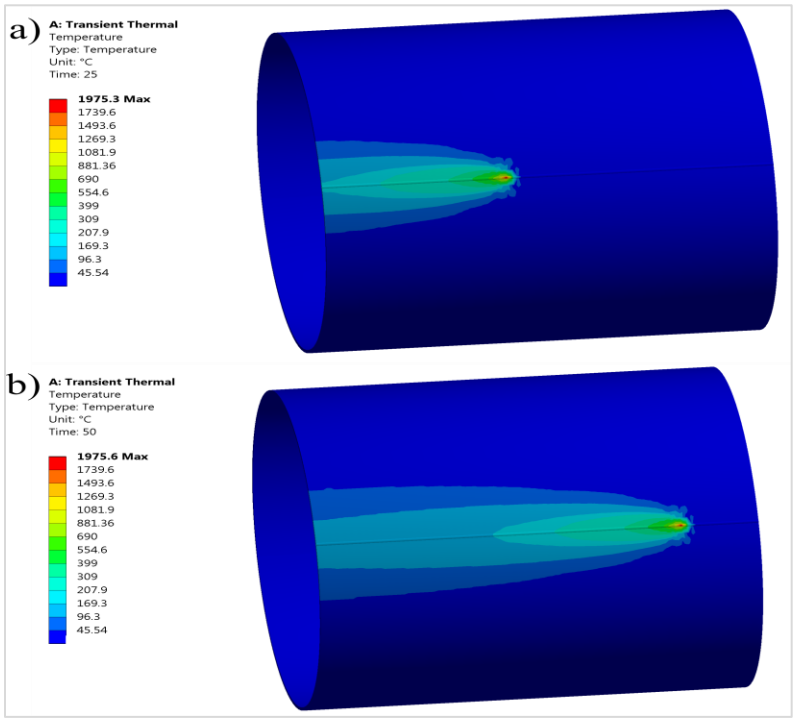

Figure 15 Temperature profiles for L-300 at two different time frames

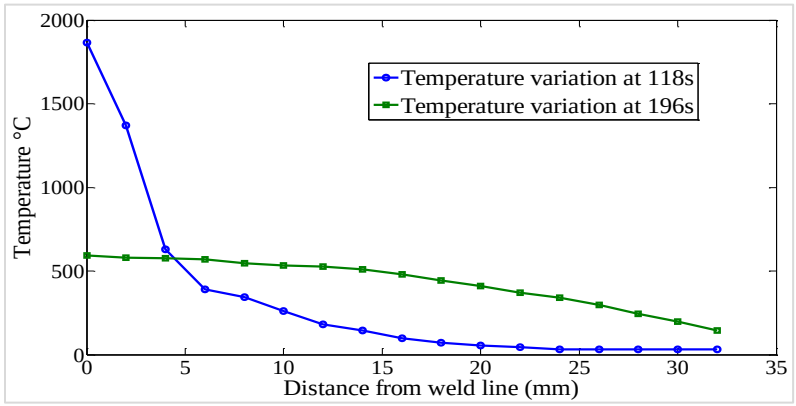

Figure 16 Temperature variation in case of C-300 at different time frames

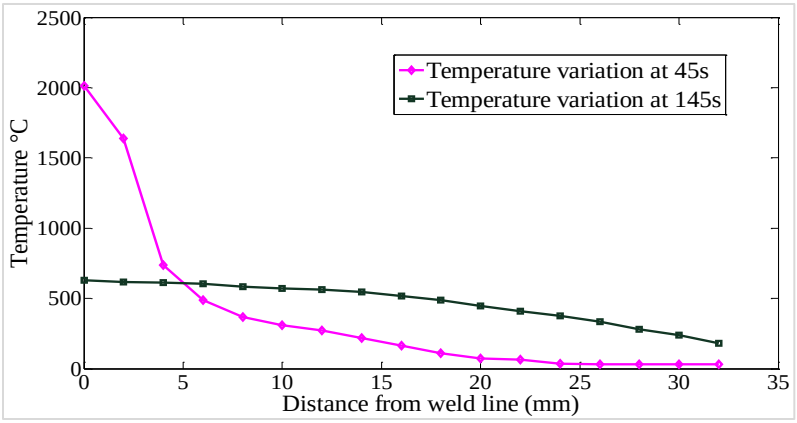

Figure 17 Temperature variation in case of L-300 at different time frame

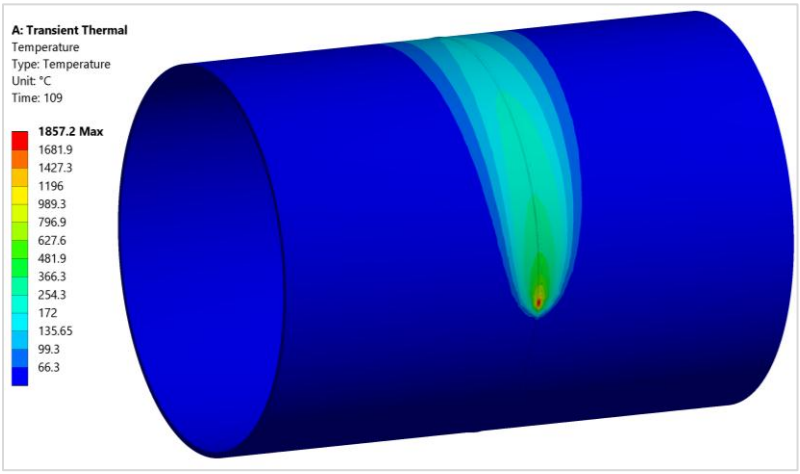

Figure 18 Temperature profile on O/S in case of C-200 at 109s

The peak temperature recorded during welding is 1857.2^0C, as shown in *Figure 18.* The temperature is maximum on the weld line because of heat source.

Figure 19 (a) and *(b)* shows the temperature variation for C-200 at two different time frames during the welding process. The maximum temperature recorded are 1855.9^0C and 1853^0C at 52s and 98s, respectively. The maximum temperatures recorded are on weld line.

In case of L-200, the heat source takes 100s to complete the welding process. The peak temperature is recorded at 45s and is as shown in the *Figure 20.*

The peak temperature recorded is 1921.4^0C and is observed on the weld line. From *Figures 18* and *20*, the peak temperature recorded in case of L-200 is higher than C-200. Peak temperature in case of L-200 is around 64^0C higher than C-200.

Figure 21 (a) and *(b)* shows the temperature variation for L-200 at two different time frames during the welding process. The maximum temperature recorded are 1921^0C and 1911.3^0C at 21s and 63s, respectively. The maximum temperatures recorded are on weld line. The gradients trailing the heat source are wider at 63s indicating heat transfer. Thus, the peak temperature recorded is higher during longitudinal welding when compared to circumferential welding.

The magnitude of peak temperatures for cases C-200 and C-300 is almost same. For the cases L-200 and L-300 a very small amount of difference is found in the magnitude of peak temperatures. Also, the peak temperatures recorded are almost at the same time frame. The time taken from the heat source to complete the welding for L-300 and L-200 are same.

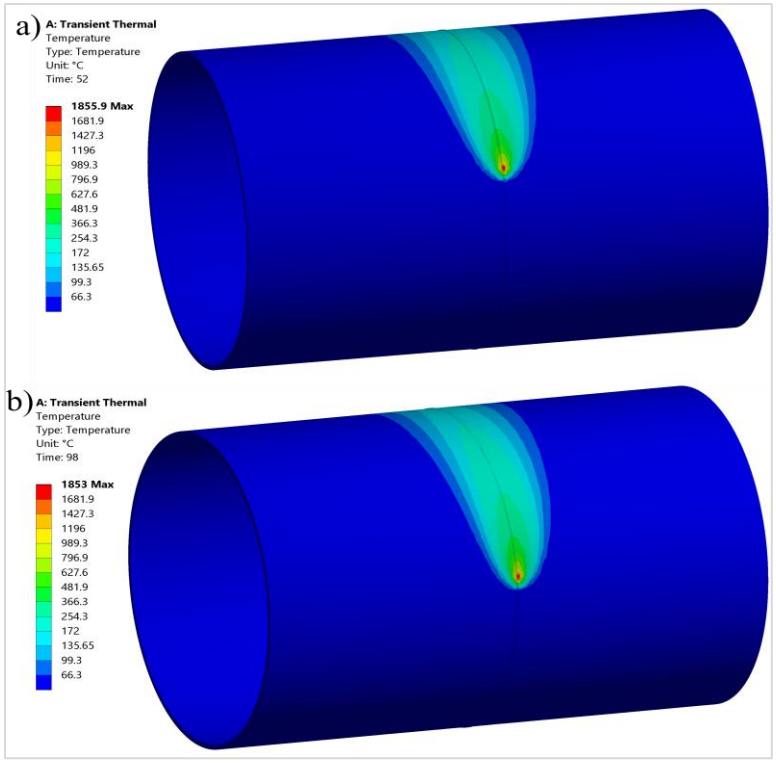

Figure 19 Temperature profiles for C-200 at two different time frames

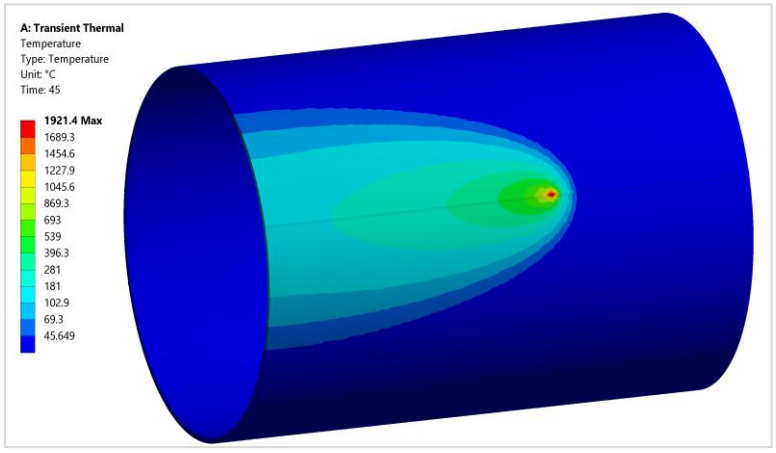

Figure 20 Temperature profile on the O/S in case of L-200 at 45s

4.3Structural analysis

For circumferential butt weld joints, stress parallel to the weld line is hoop stress, and the stress along the axis of the cylinder is axial stress. Similarly, in case of longitudinal butt weld joints, stress parallel and normal to weld line is axial and hoop stress, respectively.

Weld induced stresses are evaluated on both the I/S and O/S of the cylinder during structural analysis. The residual axial stress variations on the cylinder surfaces, for all the four cases, are shown in *Figures 22* and *23*, respectively. Similarly, residual hoop stress variations on the cylinder surfaces are shown in the *Figures 24* and *25*, respectively. The weld induced hoop and axial stress variations are evaluated at 180^0 for the cases C-300 and C-200. In cases L-300 and L-200, stress variations are considered at 150mm cross-section. It can be noted that the section 180^0 is considered circumferentially from the weld start location. The section 150mm is considered axially from the weld start location.

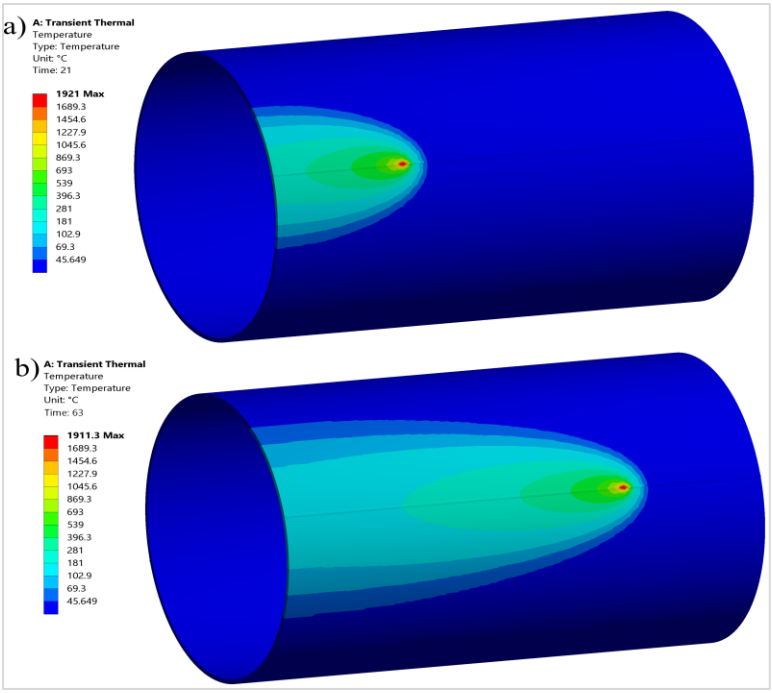

Figure 21 Temperature profiles for L-200 at two different time frames

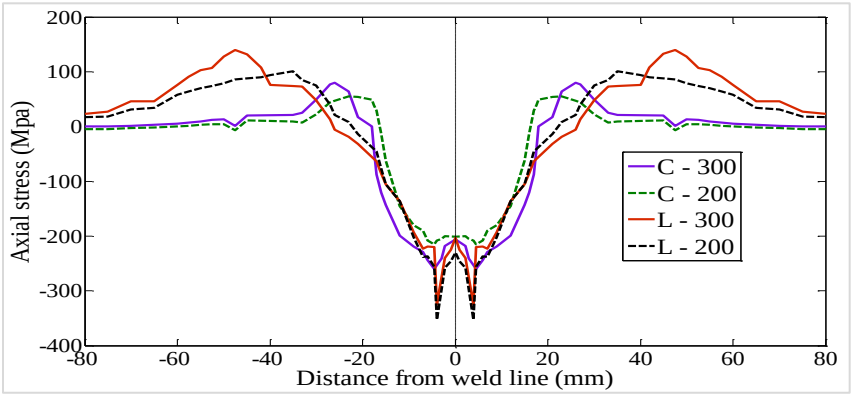

Figure 22 Weld induced axial stress distribution on the O/S of the cylinder

From the *Figure 22*, axial stress induced due to weld on the O/S of the cylinder is compressive on the weld line, for all the four cases. The stress reverses to tensile at the regions away from the weld line. Then stress gradually becomes nil at the sections which are around 80mm away from the weld line. Beyond 80mm, the magnitude of residual stresses is very small and can be neglected. From the *Figure 23*, the axial stress on the I/S of the cylinder is tensile on and near the weld line for all the four cases. The stress reverses to compressive at the regions away from the weld line. Stress almost becomes zero at the sections 75mm away from the weld line. The axial stress distribution profiles are similar in all the four cases, but significant difference can be found in their magnitudes.

The magnitude of axial stress on both O/S and I/S of cylinder in case of C-200 is lower than C-300 at all the locations. Also, the stress zone is an important parameter in considering the integrity of the cylinder vessels. Stress zone is the area until the residual stress is induced from the weld line. In case of C-200, the stress zone is compressive and extended till 18mm on either side of weld line on the O/S of the cylinder. Whereas in case of C-300 stress zone is extended till 24mm on either side of the weld line. Similarly, on the I/S, the stress zone is tensile and extended till 21mm and 27mm on either side of the

weld line for C-200 and C-300, respectively. Thus, the stress zone is smaller in the case of C-200 when compared to C-300. The magnitude of axial stress on the I/S for L-200 and L-300 are almost same at all the locations. While the magnitude of axial stress on the O/S is higher in case of L-300. The stress zone on either side of the weld line is almost same for both L-300 and L-200. The compressive stress zone on either side of the weld line for L-300 is larger than C-300 on O/S of the cylinder. While the stress zone is tensile and is almost same for both L-300 and C-300 on I/S of the cylinder.

From the *Figures 24* and *25*, it is found that the residual hoop stresses are tensile on and near the weld line, for all the four cases. The hoop stress reverses to compressive at the sections away from weld line. Stress gradually reduces to zero beyond 80mm from the weld line.

The magnitude of hoop stress on both the O/S and I/S, in case of C-300, is slightly higher than C-200. The hoop stress zone on the O/S of the cylinder is tensile and extended till 16.9mm from the weld line in case of C-200. Whereas in case of C-300 the tensile stress zone is extended till 18.3mm. Similarly, on the I/S of the cylinder, the hoop stress zone is tensile and extended till 16mm and 19mm from the weld line in case of C-200 and C-300, respectively. Thus, the hoop stress zone in case of C-200 is smaller than C-300. The magnitude of hoop stress on O/S and I/S of the cylinder for L-200 and L-300 are same at all the locations. Also, the hoop stress zones are equal. In case of L-300, the stress zone is tensile and extended till 20mm on O/S of the cylinder. Whereas on I/S of the cylinder, the stress zone is tensile and extended till 24.6mm. Thus, the stress zones for L-300 are significantly larger than C-300.

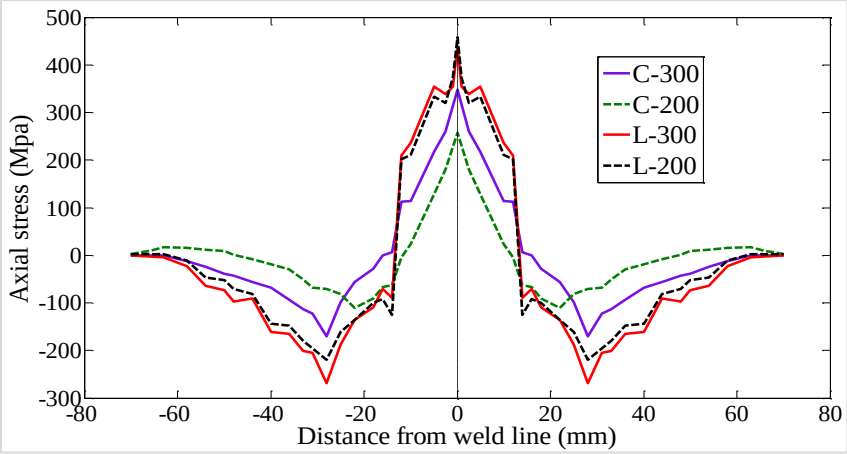

Figure 23 Weld induced axial stress distribution on the I/S of the cylinder

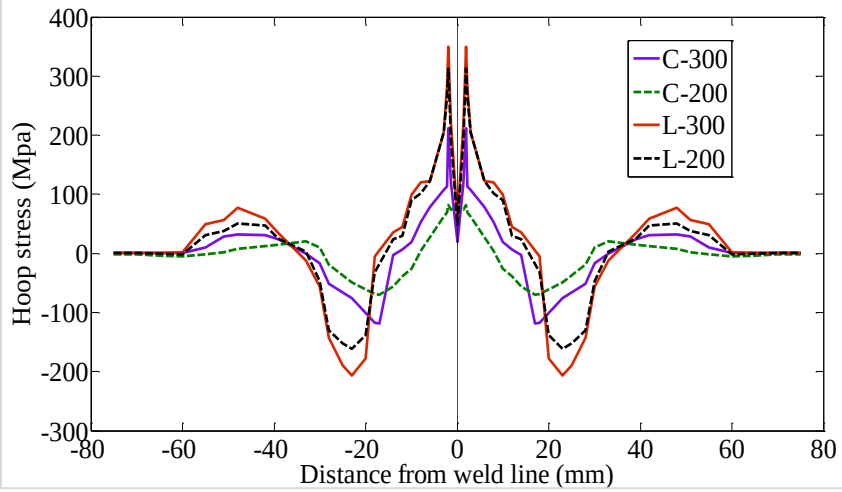

Figure 24 Weld induced hoop stress distribution on the O/S of the cylinder

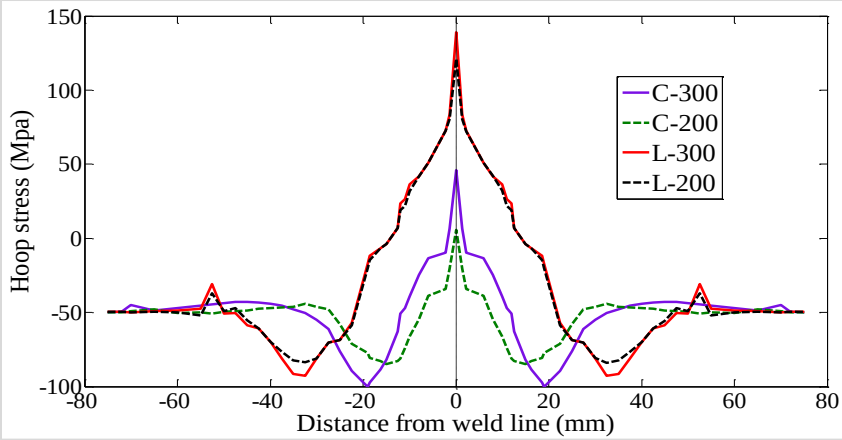

Figure 25 Weld induced hoop stress distribution on the I/S of the cylinder

It can be noted that peak hoop and axial stresses are observed in case of L-300. The magnitude of peak axial and hoop stresses are 454Mpa and 375Mpa. These peak residual stresses are tensile and found on the weld line. Also, the magnitude of hoop stresses for L-300 are 135Mpa and 185Mpa greater than C-300, on O/S and I/S of the cylinder, respectively. The magnitude of residual stresses for L-300 and L-200 is almost equal and are greater than C-300 and C-200.

5.Discussions

From the thermal analysis, it is observed that the peak temperature recorded during longitudinal welding is higher when compared to circumferential welding. The residual stress distribution profiles for all the four cases C-300, C-200, L-300 and L-200 are similar. But the magnitude of residual stresses is higher in case of L-300 and L-200. Therefore, residual stresses are higher in case of longitudinal butt weld joints than circumferential butt weld joints. The arc travel time during circumferential welding increases with an increase in the outer diameter of the cylinder. Thus, residual stress zone increases with an increasing outer diameter of the cylinder. Whereas during longitudinal welding, increasing the outer diameter does not affect the arc travel time. Because of internal pressure in the thin-walled cylinder, hoop and axial stresses are induced. The hoop stress will be two times larger in magnitude than the axial stress. This pressure induced hoop stress sums up to the residual hoop stress in case of welded cylinder vessels. Therefore, the magnitude of peak hoop stresses induced in longitudinal butt weld joint is significantly higher than circumferential butt weld joint. Thus, it can be concluded that longitudinal butt weld joints are not advisable for fabricating cylindrical component. In the present work, FE analysis is carried out on GTAW, does not consider any welding defects like undercuts, porosity and inclusions. The weld defects, affect the residual stress distribution in welded structures. A complete list of abbreviations is shown in *Appendix I.*

6.Conclusion and future work

In the present work, FE method is used to calculate the thermal histories and residual stress variation in circumferential and longitudinal butt weld joints of cylinder vessels. By observing the results following are the conclusions drawn:

1) The thermal histories and residual stress distributions for circumferential butt weld joints from the FE model, matches closely with the experimental measurements available in the literature.
2) The magnitude of peak temperatures recorded are 1865.2^0C, 1993.9^0C, 1857.2^0C and 1921.4^0C for C-300, L-300, C-200 and L-200, respectively. Therefore, peak temperature during longitudinal welding is higher than circumferential welding.
3) As the cylinder components considered for welding are of the same material, the induced residual stress profiles are similar on either side of the weld line.
4) The residual hoop stress induced in both circumferential and longitudinal weld joints is maximum near the weld line and is tensile.
5) As the outer diameter of the cylinder increases, the stress zone increases and this is because of higher bending in cylinders of larger diameter.
6) The magnitude of peak axial stresses is 435Mpa, 454Mpa, 345Mpa and 254Mpa for L-300, L-200, C-300 and C-200, respectively. Similarly, peak hoop stresses are 375Mpa, 339Mpa, 210Mpa and 112Mpa for L-300, L-200, C-300 and C-200, respectively.

The magnitude of the axial and hoop stresses is maximum in longitudinal butt weld joints. Thus, longitudinal welding is not desirable for fabricating cylinder components, as it reduces the service life. The FE model developed for GTAW can be implemented to other welding processes like Metal Inert Gas welding and Electron Beam Welding by considering minor changes according to welding. The present FE model used for low alloy steel to predict thermal histories and residual stress distributions can be used for other metals by considering its temperature dependent properties.

Acknowledgment

The Authors appreciatively acknowledge Siddaganga Institute of Technology, Tumkur for the valuable support provided for the research work.

Conflicts of interest

The authors have no conflicts of interest to declare.

Author's contribution statement

Veeresh B R: Conceptualization, investigation, data curation, writing–original draft. **R Suresh**: Conceptualization, analysis and interpretation of results. **Gowreesh S S**: Supervision, investigation on challenges and draft manuscript preparation.

References

[1] Hibbitt HD, Marcal PV. A numerical, thermo-mechanical model for the welding and subsequent loading of a fabricated structure. Computers & Structures. 1973; 3(5):1145-74.

[2] Feng Z. Processes and mechanisms of welding residual stress and distortion. Elsevier; 2005.

[3] Kermanpur A, Shamanian M, Yeganeh VE. Three-dimensional thermal simulation and experimental investigation of GTAW circumferentially butt-welded Incoloy 800 pipes. Journal of Materials Processing Technology. 2008; 199(1-3):295-303.

[4] Ueda Y, Fukuda K, Kim YC. New measuring method of axisymmetric three-dimensional residual stresses using inherent strains as parameters. Journal of Engineering Materials and Technology. 1986; 108(4):328-34.

[5] Vaidyanathan S, Todaro AF, Finnie I. Residual stresses due to circumferential welds. Journal of Engineering Material and Technology. 1973; 95(4): 233-7.

[6] Lee CH, Chang KH. Three-dimensional finite element simulation of residual stresses in circumferential welds of steel pipe including pipe diameter effects. Materials Science and Engineering: A. 2008; 487(1-2):210-8.

[7] Pandey C, Mahapatra MM, Kumar P. A comparative study of transverse shrinkage stresses and residual stresses in P91 welded pipe including plasticity error. Archives of Civil and Mechanical Engineering. 2018; 18(3):1000-11.

[8] Yaghi AH, Hyde TH, Becker AA, Sun W, Wen W, Hilson G, et al. Comparison of measured and modelled residual stresses in a welded P91 steel pipe undergoing post weld heat treatment. International Journal of Pressure Vessels and Piping. 2020.

[9] Malik AM, Qureshi EM, Dar NU, Khan I. Analysis of circumferentially arc welded thin-walled cylinders to investigate the residual stress fields. Thin-Walled Structures. 2008; 46(12):1391-401.

[10] Zhao W, Jiang W, Zhang H, Han B, Jin H, Gao Q. 3D finite element analysis and optimization of welding residual stress in the girth joints of X80 steel pipeline. Journal of Manufacturing Processes. 2021; 66:166-78.

[11] Wu C, Kim JW. Analysis of welding residual stress formation behavior during circumferential TIG welding of a pipe. Thin-Walled Structures. 2018; 132:421-30.

[12] Golikov NI. Effect of residual stress on crack development in longitudinal welded joints of a gas pipeline. Procedia Structural Integrity. 2020; 30:28-32.

[13] Obeid O, Alfano G, Bahai H, Jouhara H. Numerical simulation of thermal and residual stress fields induced by lined pipe welding. Thermal Science and Engineering Progress. 2018; 5:1-14.

[14] Liu Y, Wang P, Fang H, Ma N. Characteristics of welding distortion and residual stresses in thin-walled pipes by solid-shell hybrid modelling and experimental verification. Journal of Manufacturing Processes. 2021; 69:532-44.

[15] Lee JH, Jang BS, Kim HJ, Shim SH, Im SW. The effect of weld residual stress on fracture toughness at the intersection of two welding lines of offshore tubular structure. Marine Structures. 2020.

[16] Taghipour M, Bahrami A, Mohammadi H, Esmaeili V. Root cause analysis of a failure in a flange-pipe welded joint in a steam line in an ammonia plant: experimental investigation and simulation assessment. Engineering Failure Analysis. 2021.

[17] Mirzaee-sisan A. Welding residual stresses in a strip of a pipe. International Journal of Pressure Vessels and Piping. 2018; 159:28-34.

[18] Asadi P, Alimohammadi S, Kohantorabi O, Fazli A, Akbari M. Effects of material type, preheating and weld pass number on residual stress of welded steel pipes by multi-pass TIG welding (C-Mn, SUS304, SUS316). Thermal Science and Engineering Progress. 2020.

[19] Kumar P, Kumar R, Arif A, Veerababu M. Investigation of numerical modelling of TIG welding of austenitic stainless steel (304L). Materials Today: Proceedings. 2020; 27:1636-40.

[20] Khoshroyan A, Darvazi AR. Effects of welding parameters and welding sequence on residual stress and distortion in Al6061-T6 aluminum alloy for T-shaped welded joint. Transactions of Nonferrous Metals Society of China. 2020; 30(1):76-89.

[21] Liu RF, Wang JC. Finite element analyses of the effect of weld overlay sizing on residual stresses of the dissimilar metal weld in PWRs. Nuclear Engineering and Design. 2021.

[22] Dai P, Wang Y, Li S, Lu S, Feng G, Deng D. FEM analysis of residual stress induced by repair welding in SUS304 stainless steel pipe butt-welded joint. Journal of Manufacturing Processes. 2020; 58:975-83.
[23] Liu C, Lin C, Liu W, Wang S, Chen Y, Wang J, et al. Effects of local ultrasonic impact treatment on residual stress in an engineering-scale stainless steel pipe girth weld. International Journal of Pressure Vessels and Piping. 2021.
[24] Sidorov MM, Golikov NI, Saraev YN. Redistribution of residual stresses in girth weld of a pipe of strength class K60 after ultrasonic impact treatment. Procedia Structural Integrity. 2020; 30:149-53.
[25] Ren S, Li S, Wang Y, Deng D, Ma N. Finite element analysis of residual stress in 2.25 Cr-1Mo steel pipe during welding and heat treatment process. Journal of Manufacturing Processes. 2019; 47:110-8.
[26] Goldak J, Chakravarti A, Bibby M. A new finite element model for welding heat sources. Metallurgical Transactions B. 1984; 15(2):299-305.
[27] Goldak JA, Akhlaghi M. Computational welding mechanics. Springer Science & Business Media; 2005.

Veeresh B R is an Assistant Professor at JSS Academy of Technical Education, Bangalore. He earned his B.E. degree in Mechanical Engineering from Siddaganga Institute of Technology, Tumkur and M.tech in Machine Design from UBDT college of Engineering, Davanagere. He is pursuing his Ph.D in Mechanical Engineering. He is a member of the Fluid Power Society of India (FPSI). He has guided six UG projects, among which two projects were funded from Karnataka State Council for Science and Technology (KSCST), Bangalore. He has six years of experience in teaching and has published five papers in peer reviewed journals.
Email: v.veereshbr@gmail.com

Dr. R Suresh is a Professor at Siddaganga Institute of Technology, Tumkur. He is a coordinator for District Bio Fuel Information & Demonstration funded by Karnataka State Bio-Fuel Development Board. He has carried out one project funded from Vision Group on Science and Technology (VGST) and six projects funded from Karnataka State Council for Science and Technology (KSCST). He is a life member of Indian Society for Technical Education, Indian Institute of Metals and Society for Failure Analysis. Three Research scholars are awarded Ph.D under his guidance and three Research scholars are pursuing Ph.D under his guidance. He has 36 years of teaching experience and has published 32 papers in peer reviewed journals.
Email: suresh_tumin@yahoo.co.in

Dr. Gowreesh S S is an Associate Professor at JSS Academy of Technical Education, Bangalore. He has 12 years of Industrial experience and has worked in Philips Advanced Technology Center, Netherlands, WorleyParsons India Private Limited and CYIENT, formerly called Infotech Enterprises Limited. He has expertise in CFD modelling and Analysis using CAE Packages CFX, FLUENT and ANSYS Workbench. He has carried out one project funded from the Scheme for Promoting Interests, Creativity and. Ethics among Students (SPICES), AICTE and nine projects funded from Karnataka State Council for Science and Technology (KSCST). Four Research scholars are pursuing Ph.D under his guidance. He has six years of experience in teaching and has published 30 papers in peer reviewed journals.
Email: gowreesh.ss@gmail.com

Appendix I

S. No.	Abbreviation	Description
1	^{0}C	Degree Celsius
2	A	Ampere
3	amb	Ambient
4	CAD	Computer-aided design
5	D	Dimensional
6	FE	Finite Element
7	GTAW	Gas Tungsten Arc Welding
8	I/S	Inner Surface
9	J	Joule
10	K	Kelvin
11	m	Meter
12	mm	Millimeter
13	Mpa	Mega pascal
14	O/S	Outer Surface
15	U_x	Displacement in x-Coordinate
16	U_y	Displacement in y-Coordinate
17	U_z	Displacement in z-Coordinate
18	V	Volt
19	W	Watt